Supporting Information

Effect of Confinement on the Exciton and Bi-exciton Dynamics in Perovskite 2D-Nanosheets and 3D-Nanocrystals

Ayushi Shukla[§, ‡], Gurpreet Kaur[§, ‡], K. Justice Babu[§], Nandan Ghorai[§], Tanmay Goswami[§], Arshdeep Kaur[§], and Hirendra N. Ghosh[†§*]

[§]Institute of Nano Science and Technology, Mohali, Punjab -160062, India.

[†]Radiation and Photochemistry Division, Bhabha Atomic Research Centre, Mumbai -400085, India.

[‡]Both the authors contributed equally.

I. Experimental details

1) Synthesis:

The colloidal $CsPbBr_3$ NCs[1] and NSs[2] were synthesized following a previously reported synthesis methodology with minor modifications.

Chemicals and reagents: Cesium carbonate (Cs_2CO_3, 99 % trace metals basis), Lead (II) bromide ($PbBr_2$, 99.99 % trace metals basis), Oleylamine (OLA, tech, 70 %), Oleic acid (OA, tech, 90%), 1-octadecene (ODE, tech, 90%) were purchased from Sigma-Aldrich and used without further purification. Anhydrous DCM (AR grade) was used to purify the crude product, and n-hexane was used to disperse the purified samples for further characterizations.

Synthesis of $CsPbBr_3$ NCs and NSs:

1. **Preparation of Cs-Oleate**:

Three-neck round-bottomed flask 1.25mmol (~0.41 g) Cs_2CO_3, 20 mL of ODE, and 4 mmol OA (~1.4 mL) were loaded in a50 mL and the mixture was continuously stirred

undervacuum for 30 min at 120 °C, then the mixture in the flask was purged under N_2 for 10 min and again placed under vacuum. The process was repeated to remove any dissolved $O_2$and moisture from the flask. Then the mixture was heated at 150 °C for the complete dissolution of Cs_2CO_3 under N_2 atmosphere. The complete dissolution of the Cs_2CO_3 indicates the formation of the Cesium oleate. The temperature of the obtained Cs-oleate solution was maintained above 100 °C before usage for the synthesis of Nanocrystals and Nanosheets.

2. $CsPbBr_3$ NCswas synthesized after following the synthetic method reported by Kovalenko and co-workers[1] with minor modifications. $PbBr_2$ (0.188 mmol), ODE (5 mL), OA (0.7mL) and OLA (0.7 mL) were mixed in a 25 mL 3-neck round-bottomed (RB) flask, and mixture was stirred under vacuum for 30 min at 120 °C, then the flask was purged under N_2 for 5 mins. Then, the temperature was increased to 160 ºC and Cs-oleate (~0.4 mL) solution was quickly injected. Within 10sec, the reaction mixture was cooled in an ice-cold water bath and the crude solution was further centrifuged at 10000rpm for 10 mins to remove the unreacted precursors. The supernatant obtained after centrifuge was removed and the obtained NCs were dispersed in n-hexane.

3. $CsPbBr_3$ NSswassynthesizedafter following the synthetic method reported by lv and co-workers[2]with minor modifications. In a three-neck RB flask, 69 mg of $PbBr_2$ (0.188 mmol), 5 mL of ODE, 0.7 mL of OA, and 1.4 mL of OAm were loaded and dried under vacuum at 120 °C for 1 h. After that, the temperature was raised to 140 °C, at which 0.5 mL of the Cs-oleate precursor was swiftly injected into the reaction mixture. The reaction was maintained at the desired temperature for 30 min and then quenched by an ice-cold water bath. The crude solution was dissolved with 5 mL of anhydrous DCM, and then centrifugation was carried out at 10000 rpm for 10 min. The supernatant was discarded and the precipitated nanosheets were re-dispersed in 5 mL of anhydrous n- hexane to form a

stable colloidal dispersion, which is generally stable without precipitation for months when stored in the glovebox.

II. Instrumentation details

The morphological studies of the synthesized NCs and NSswere done by using Transmission Electron Microscope (TEM, JEOL JEM 2100) functioning at an accelerating voltage of 200 kV. The XRD patterns of prepared NCs and NSswere determined through a powder X-ray diffractometer (BRUKER D8 ADVANCE) with Cu-Kα radiation (λ = 1.542 Å) running with a scanning angle (2θ) range of 10-50^{o}. The steady state absorption studies were performedwith a Shimadzu UV-2600 UV-vis spectrophotometer. The Fluorescence measurements were carried out using Edinburgh FS5 spectrofluorometer instrument. The photoluminescence decay lifetimes were performed by time-correlated single-photon counting (TCSPC) technique with a Delta flex Modular Fluorescence Lifetime System (HORIBA Scientific) with Nano-LED pulsed diode light source (402 nm).The instrument response function (IRF) was recorded using Ludox (colloidal silica) solution up to 200 ps.The NCs and NS were dispersed in n-hexane during all the experiments conducted.

Femtosecond Pump-Probe Spectrometer:

The femtosecond transient absorption measurements of $CsPbBr_3$ NCs and NSs were carried out usingHelios Fire Spectrometer. The setup consists of a Helios Fire spectrometer, Ti: Sapphire regenerative amplifier-based femtosecond laser system (Astrella, Coherent systems) which is having central wavelength ~800 nm, Pulse energy ~2 mJ and ~35 fs pulse width.The detailed explanation is provided in our previously reported articles.[3]The pump probe spectroscopy includes two beams a pump and a probe. A dichroic beam splitter is used to divide the pump beam with therepetition rate (1 kHz) into two components as a pump and probe beam (R:T = 90:10). The Optical Parametric Amplifier (OPerA-SOLO, model no. TO8U6WS)) is

used to tune the pump beamto any essential excitation wavelength within the limits defined by the system. Neutral density (ND) filters are used in order to vary the intensity of pump beam. The probe beam is incident on a sapphire crystal to producecontinuum of white light. The sample is magnetically stirred all along the duration of the experiment to avoid the photo charging effects. The data analysis was done using Surface Explorer software.

III. XRD details

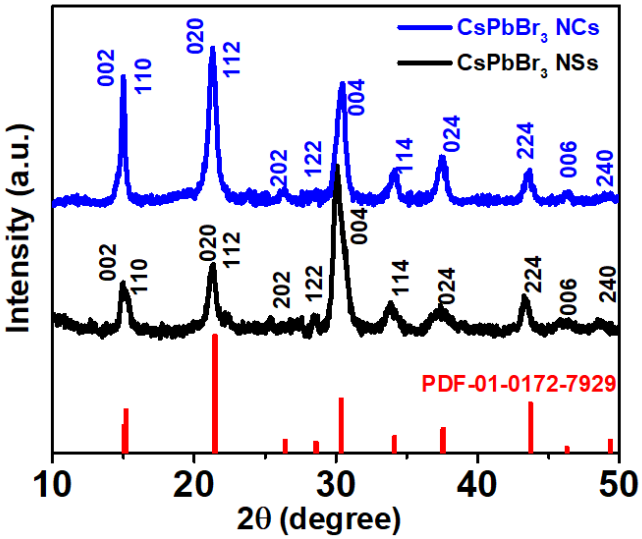

Figure S1: XRD patterns of $CsPbBr_3$ NCs and NSs.

The X-Ray Diffraction (XRD) patterns of as synthesized $CsPbBr_3$ nanocrystals and nanosheets are depicted in figure S1. The XRD peaks are well defined and are in good agreement with the reported JCPDS Values (PDF-01-0172-7929).[4]The XRD studies reveal that both in the case of $CsPbBr_3$ NCs and NSs the orthorhombic phase of the $CsPbBr_3$ is maintained.

IV. Time Resolved Photoluminescence (TRPL) Studies:

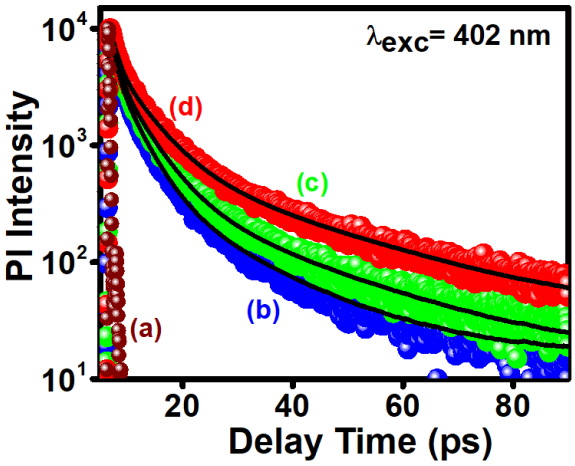

Figure S2: TRPL measurements for (a) IRF(b,c) $CsPbBr_3$ NS corresponding to emission wavelength at 476 and 490 nm respectively, and (d) $CsPbBr_3$ NCs for emission wavelength at 516 nm. The samples were excited at 402 nm.

Figure S2 shows the TRPL measurements for both $CsPbBr_3$ NCs and NSwhenexcited at 402nm.Interestingly, the peak intensity at 490 nm is much higher as compared to that at 476 nm, which can be attributed to the de-population of the LH band as a consequence of the hole moving towards the HH band. We carried out time-resolved PL measurements (TRPL) to further monitor the lifetimes associated with these transitions in both the materials under study (Excitation wavelength = 402 nm).PL lifetime for $CsPbBr_3$ NCs is determined to be 4.6 ns. However for NSs, it is found to be 2.35 ns and 3.01 ns when monitored at 476 nm and 490 nm respectively (Figure S2). The comparatively shorter PL lifetime obtained for NSs can be attributed mainly due to increased quantum confinement in these materials, which enhances the overlapping between the carrier wave functions, leading to faster recombination.[5] Additional factor that can be held liable for this reduced PL lifetime is the higher surface trap state density and in 2D NSs[6]. Similar effect of dimensionality was observed by Zhang *et.al*[5] in $CsPbBr_3$ NCs and nanoplatelets.[5]

V. Recombination kinetics for both the $CsPbBr_3$ NCs as well as NSs:

The linear behaviour of ΔA^{-2} vs. delay time, clearly suggests that the bi-excitonic Auger recombination is dominating process occurring during the initial bleach recovery time scale. Correspondingly, during the long probe delays, the linear behaviour of ΔA^{-1} vs. delay time t recommends that the excitonic recombination process is dominant.[4]

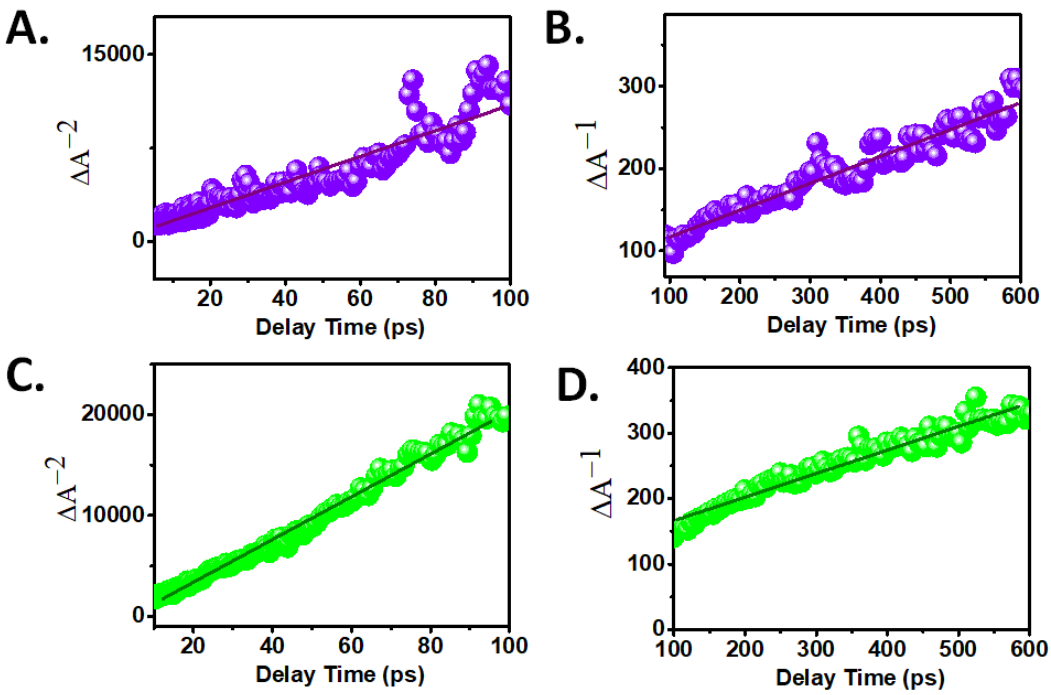

Figure S3. (A,C) depicts the linear dependence of ΔA^{-2} vs. early probe delay implying the Auger biexcitonic recombination mode in $CsPbBr_3$ NCs and NSs respectively for 300 nm excitation. (B,D) shows the linear dependence of ΔA^{-1} vs. delay timein $CsPbBr_3$ NCs and NSs respectively inferring the radiative recombination is dominating at this time span for 300 nm excitation.

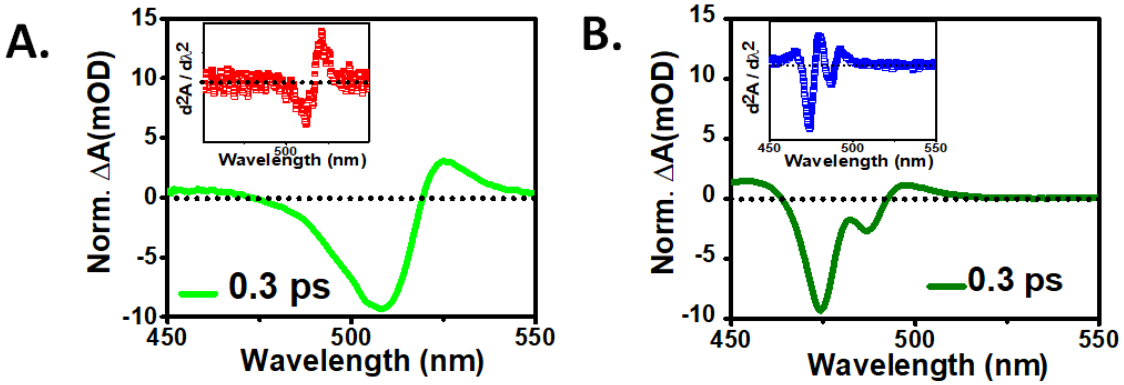

Figure S4:(A,B) Early time (0.3 ps) TA spectra of $CsPbBr_3$ NC and $CsPbBr_3$ NSs matches with the second derivative of steady-state absorption for $CsPbBr_3$ (inset), which clearly signifies the biexciton-induced Stark effect in the TA spectra.

The origin of derivative-like feature in the transient absorption data at the early time scale forthright the excitation in both the systemsFigure S4(A,B).Transient Absorption spectra at initial time delays is identical to the second order derivative of the absorption spectra (Figure S4 A,B inset).This observation clearly supports the biexcitonic induced stark effect in both the systems.[7]

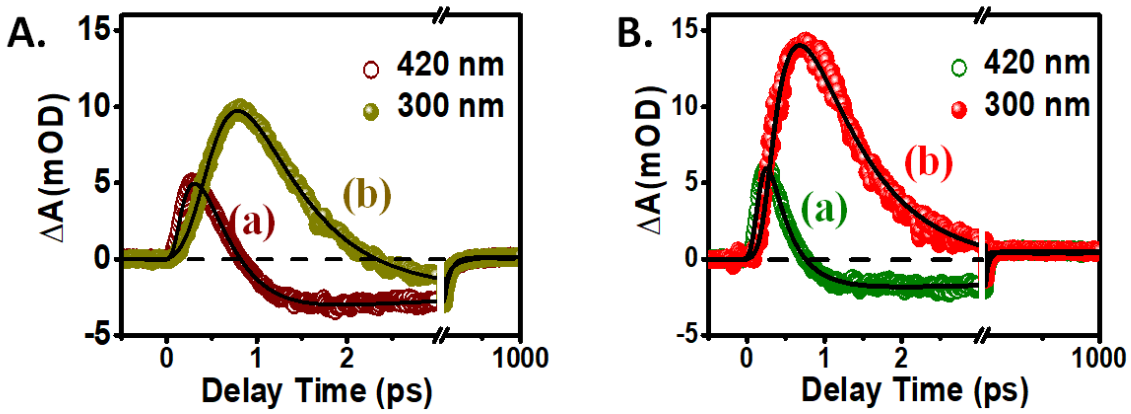

Figure S5. (A) Kinetic traces for $CsPbBr_3$ NCs probed at probe wavelength λ = 525 nm at (a) 420 nm and (b) 300 nm pump excitation. **(B)**Kinetic traces for $CsPbBr_3$ NSs probed at probe wavelength λ = 498nm (positive band) for both(a) 420 nm and (a) 300 nm pump excitation.

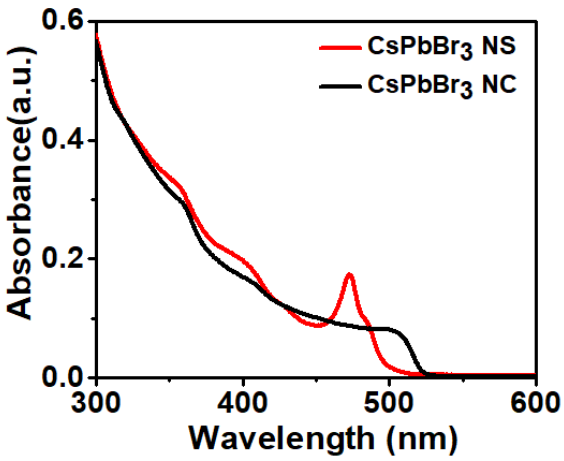

Figure S6. Comparative Optical absorbance spectra for $CsPbBr_3$ NCs and NSs.

Table S1. Kinetics Fitting Parameters for $CsPbBr_3$ NCs Dispersed in n-hexane after exciting the Samples at 420 nm and 300 nm.

		Probe wavelength	τ_{growth}	τ_1	τ_2	τ_3	τ_4
$CsPbBr_3$ NCs	**420 nm pump excitation**	**510 nm**	τ_1^g =< 100 fs(35%) τ_2^g =460 fs (65%)	8ps (-32.68%)	42ps (-31.5%)	211ps (-22.62%)	>1ns (-13.2%)
	300 nm pump excitation	**510 nm**	τ_1^g =190fs (54%) τ_2^g =1.18ps (46%)	4.42ps (-28%)	25.25ps (-44%)	162ps (-20%)	>1ns (-7.38%)

Table S2. Kinetics Fitting Parameters for $CsPbBr_3$ NSs at different wavelengths dispersed in n-Hexane after Exciting the Samples at 420 nm.

	Probe wavelength	Bleach growth	Recovery				
			τ_1	τ_2	τ_3	τ_4	τ_5
CsPbBr3 NSs	**474nm**	τ_1^g=< 100 fs(100%)	310 fs (-7.3%)	2.21ps (-24.2%)	66.3ps (-45.75%)	150ps (-11.2%)	>1ns (-11.55%)
	487 nm	τ_1^g=330fs (100%)	3.37ps (-28.1%)	78ps (-47%)	161ps (-12.1%)	>1ns (-12.8%)	

Table S3. Kinetics Fitting Parameters for $CsPbBr_3$ NSs Dispersed in n-Hexane after Exciting the Samples at 300 nm.

	Probe wavelength	Transient growth	Bleach growth	Recovery		
				τ_1	τ_2	τ_3
$CsPbBr_3$ NSs	**400 nm**		τ_1^g=100fs (100%)	7.2ps (81.3%)	45ps (16.2%)	>1ns (2.5%)
	474 nm		τ_2^g=320fs (100%)	15.5 ps (75.2%)	440ps (21.4%)	>1ns (3.4%)
	487 nm	$\tau_{g\,1}$ =< 100 fs (25.6%) τ_{d1}=158 fs (-32%)	τ_1^g=835fs (-68%)	38.75ps (58.5%)	465 ps (11.7%)	>1ns (4.2%)

Table S4. Kinetics Fitting Parameters for $CsPbBr_3$ NCs and NSs dispersed in n-Hexane after Exciting the Samples at 300 nm and 420 nm respectively.

	pump λ_{nm}	Probe λ_{nm}	(biexciton) Growth τg_b	(biexciton) decay	(single exciton)			
					growth	recovery		
						τ_1	τ_2	τ_3
$CsPbBr_3$ NCs	**420**	**527**	< 100 fs (62.68%)	150 fs (-62.8%)	0.485 ps (-37.2)	2.4 ps (17.7%)	51ps (15.42%)	>1ns (4.2%)
	300	**527**	210 fs (78.6%)	550 fs (-78%)	2.4 ps (-22%)	30ps (16.8%)	>1ns (4.6%)	
$CsPbBr_3$ NSs	**420**	**498**	< 100 fs (70.3%)	160 fs (-71%)	0.460 ps (-29%)	2.3 ps (11.4%)	35 ps (15.2%)	>1ns (3.1%)
	300	**498**	160 fs (89.45%)	0.730ps (-90.4%)	1.89 ps (-9.6%)	25.5ps (7.43%)	>1ns (3.12%)	

REFERENCE:

(1) Protesescu, L.; Yakunin, S.; Bodnarchuk, M. I.; Krieg, F.; Caputo, R.; Hendon, C. H.; Yang, R. X.; Walsh, A.; Kovalenko, M. V. Nanocrystals of Cesium Lead Halide Perovskites ($CsPbX_3$, X = Cl, Br, and I): Novel Optoelectronic Materials Showing Bright Emission with Wide Color Gamut. *Nano Lett.* **2015**, *15* (6), 3692–3696.

(2) Lv, L.; Xu, Y.; Fang, H.; Luo, W.; Xu, F.; Liu, L.; Wang, B.; Zhang, X.; Yang, D.; Hu, W.; Dong, A. Generalized Colloidal Synthesis of High-Quality Two-Dimensional Cesium Lead Halide Perovskite Nanosheets and Their Applications in Photodetectors. *Nanoscale* **2016**, *8* (28), 13589–13596.

(3) Ghorai, N.; Ghosh, H. N. Ultrafast Plasmon Dynamics and Hole-Phonon Coupling in NIR Active Nonstoichiometric Semiconductor Plasmonic $Cu_{2-x}S$ Nanocrystals. *J. Phys. Chem. C* **2019**, *123* (46), 28401–28410.

(4) Kaur, G.; Justice Babu, K.; Ghorai, N.; Goswami, T.; Maiti, S.; Ghosh, H. N. Polaron-Mediated Slow Carrier Cooling in a Type-1 3D/0D $CsPbBr_3$@Cs_4PbBr_6 Core-Shell Perovskite System. *J. Phys. Chem. Lett.* **2019**, *10* (18), 5302–5311.

(5) Zhang, X.; Gao, X.; Pang, G.; He, T.; Xing, G.; Chen, R. Effects of Material Dimensionality on the Optical Properties of $CsPbBr_3$ Nanomaterials. *J. Phys. Chem. C* **2019**, *123* (47), 28893–28897.

(6) Liu, N.; Liu, P.; Zhou, H.; Bai, Y.; Chen, Q. Understanding the Defect Properties of Quasi-2D Halide Perovskites for Photovoltaic Applications. *J. Phys. Chem. Lett.* **2020**, 3521–3528.

(7) Aneesh, J.; Swarnkar, A.; Kumar Ravi, V.; Sharma, R.; Nag, A.; Adarsh, K. V. Ultrafast Exciton Dynamics in Colloidal $CsPbBr_3$ Perovskite Nanocrystals: Biexciton Effect and Auger Recombination. *J. Phys. Chem. C* **2017**, *121* (8), 4734–4739.